www.dergipark.gov.tr
ISSN:2148-3736
El-Cezerî Fen ve Mühendislik Dergisi
Cilt: 5, No: 3, 2018 (773-784)

El-Cezerî Journal of Science and Engineering
Vol: 5, No: 3, 2018 (773-784)
DOI : 10.31202/ecjse.423855

ECJSE

Research Paper / Makale

Developer Effects of Pre-Heating Applied to the Al7039 Armor Plates Prior to the Friction Stir Welding

Uğur AVCI[a], Şemsettin TEMİZ[b]

[a]Kahramanmaraş Sütçü İmam University, Technical Sciences Vocational High School, Department of Machine, Kahramanmaraş 46100, Turkey
[b]İnönü University, Department of Mechanical Engineering, Malatya 44280, Turkey
ogrtmugav@gmail.com, semsettin.temiz@inonu.edu.tr

Received/Geliş: 15.04.2018 **Revised/Düzeltme:** 31.08.2018 **Accepted/Kabul:** 03.09.2018

Abstract: In this study, Al7039 plates at certain dimensions were first joined via friction stir welding (FSW) method at room temperature. During this process, thermocouple tips positioned closely to the each side of the weld helped determine temperatures on the advancing and retreating sides. These temperature values were used to estimate pre-heating temperature of the base metal prior to the welding process. After Al7039 plates at identical dimensions were heated to a certain temperature, they were joined using the same welding parameters, and the heat distribution was determined thanks to the thermocouples positioned on the same zones. The heat distribution between two samples which were joined using different heat inputs were analyzed to reveal the impact of this heat distribution on the weld zone via mechanical tests and micro structure images.

Key words : Al7039 alloy, FSW, Pre-heating

Al7039 Zırh Plakalarına Sürtünme Karıştırma Kaynağı Öncesi Uygulanan Ön Isıtmanın Geliştirici Etkileri

Öz: Bu çalışmada, belirlenen boyutlarda hazırlanan Al7039 levhalar, öncelikle oda sıcaklığında sürtünme karıştırma kaynağı yöntemi ile birleştirildi. Birleştirme esnasında kaynak başlangıç ve bitiş noktalarına yakın bölgelere yerleştirilen termokupl uçları sayesinde ilerleme kenarı ve yığılma kenarında oluşan sıcaklıklar belirlendi. Elde edilen sıcaklık değerleri kullanılarak kaynak öncesi ana metalin ön ısıtma sıcaklığı tahmin edildi. Aynı boyutlarda hazırlanan Al7039 levhalar belirlenen ön ısıtma sıcaklığına kadar ısıtıldıktan sonra aynı kaynak parametreleri ile birleştirildi ve kaynak sırasında aynı bölgelere yerleştirilen termokupllar vasıtasıyla ısı dağılımları belirlendi. Farklı ısı girdileri ile birleştirilen iki numune arasındaki ısı dağılımı incelenerek, bu ısı dağılımının kaynak bölgesindeki etkileri mekanik testler ve mikro yapı görüntüleri ile ortaya konuldu.

Anahtar kelimeler: Al7039 alaşımı, SKK, Ön ısıtma

1. Introduction

Although technological developments bring about new areas of use for the existing materials, high quality materials which can offer solutions to common problems are still needed. Therefore, it is of vital importance to improve existing materials or produce new alternative products in this process. Aluminum and its alloys are favorable engineering materials due to their low cost, low density, effective cooling, easy production and high endurance. Thanks to their high endurance, 7xxx Al-Zn-Mg alloys, which can be hardened through aging methods, are widely used in structures under

How to cite this article
Avcı U., Temiz Ş., "*Developer Effects of Pre-Heating Applied to the Al7039 Armor Plates Prior to the Friction Stir Welding"*, El-Cezerî Journal of Science and Engineering, 2018, 5(3); 773-784.

Bu makaleye atıf yapmak için
Avcı U., Temiz Ş., *"Al7039 Zırh Plakalarına Sürtünme Karıştırma Kaynağı Öncesi Uygulanan Ön Isıtmanın Geliştirici Etkileri"*, El-Cezerî Fen ve Mühendislik Dergisi 2018, 5(3); 773-784.

tough working conditions [1]. Al7039 alloys can be particularly distinguished by their high strength and energy absorption capacities, and are widely used in defense industry as an armor material [2]. Avcı and Temiz used an Al7039 alloy material as a matrix to produce functionally graded composite material and thus proposed a new approach for the production of armor materials [3]. The content of Al7039 is given in Table 1 [4].

Table 1. The content of 7039 aluminum alloy

Mg	Zn	Mn	Cr	Si	Fe	Cu	Ti	Al
2.3 -3.3	3.5-4.5	0.10-0.40	0.15-0.25	0.30 max	0.40 max	0.10 max	0.10 max	Balance

FSW is a non-fusion welding technique which remarkably eliminates problems related to the fusion welding techniques. As shown in Fig. 1, FSW method is applied by penetrating the materials along the joint line between two plates through a specially designed welding set and, at the same time, creating heat of friction thanks to rotation speed. Thus, these materials are joined through plasticization [5]. The rotation of the welding set pin in the material causes the plasticized material to retreat towards the direction of rotation, which is the weld zone called retreating side. On the other hand, the weld zone which forms as the welding set advances is called advancing side.

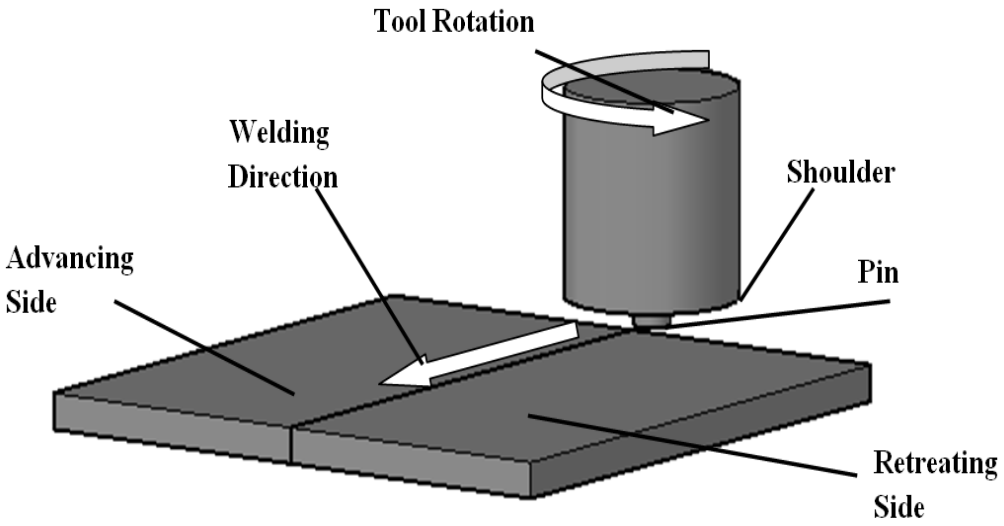

Figure 1. Friction stir welding schematic application

FSW displays a successful performance in terms of joining aluminum and its alloys which are otherwise very difficult to join using conventional welding techniques [6]. As far as aluminum and its alloys are concerned, it is possible to encounter numerous studies on material flowing during FSW [7,8], improvement of mechanical and micro structure properties [9,10] and impact of welding parameters [11,12]. Some researchers analyzed the impact of base metal heat treatment on mechanical properties and micro structure before aluminum and its alloys are joined via FSW [13,14]. Chen et al. found out that base metal heavily influenced weld structure and defects, tensile properties and fracture points after AA2219 alloy was annealed and subjected to T6 heat treatment [15]. Yan et al. underlined the impact of heat treatment applied to AA7050 base metal on mechanical properties prior to FSW [16]. However, the number of studies on FSW performed during the determination of base material heat input through heat treatment is limited. In their study on the same topic, Poongkundran and Senthilkumar observed that tensile strength and joint impact improved if base metal is welded after it is heated up to 100^{o}C [17].

2. Material and Method

In this study, as shown in Fig. 2, Al7039 alloy plates at a dimension of 80x100x5 mm^3 were positioned on a fixing apparatus. Within the framework of the numbering system shown in Fig. 3, thermocouple tips were positioned in two holes of 10 mm depth at a distance of 20 mm on the start and end of weld zones in order to monitor heat changes during FSW at room temperature. The fixing apparatus on which plates were positioned was tied to a vertical-type universal milling machine. The welding set was produced as two pieces comprising of a 30 mm shoulder and 4 mm reverse pin. After welding set rotation and advancing speed was set at 1500 rev/min and 25 mm/min, the pin penetrated the material until the shoulder touched it. Temperature values were recorded from the period when the stir pin touched Al7039 alloy material until the welding process ended. After other Al7039 alloy plates at identical dimensions were tied to the fixing apparatus, they were annealed in the oven for pre-heating. The materials which were put on the bench following pre-heating were joined using the same welding parameters, and, during this process, temperature values were recorded thanks to the thermocouples at the same points.

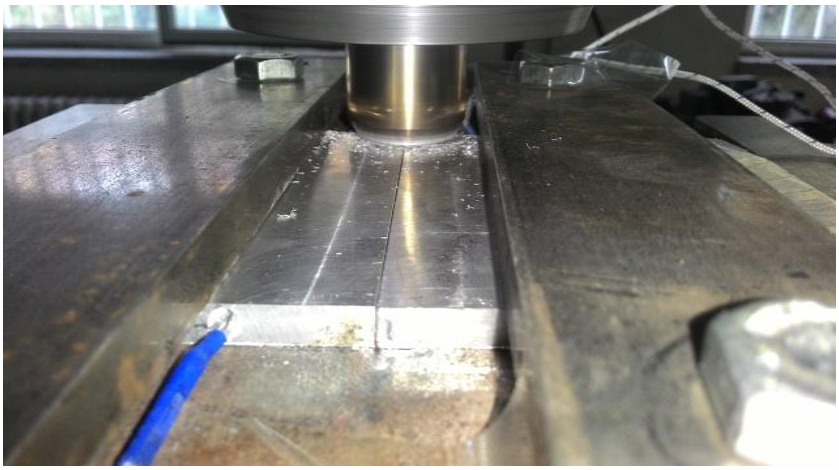

Figure 2. Material positioning during welding

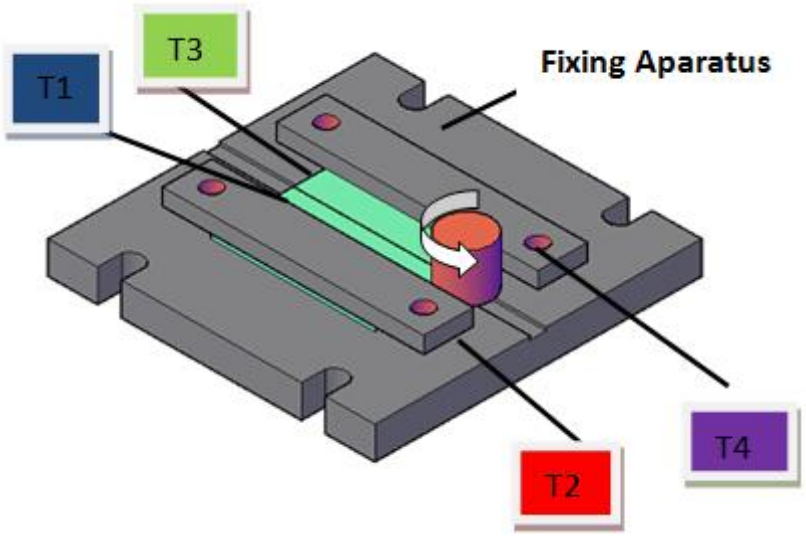

Figure 3. Thermocouple positioning

The joined samples were transversally cut at different points for metallurgical analysis. Following grinding and polishing procedures, they were cauterized in Keller chemical (1 ml HF, 1.5 ml HCl, 2,5ml HNO_3, 95 ml H_2O). Their micro-hardness values were measured via an optical microscope on

LEICA DM4000M and a load of 100 gr on Shimadzu GMV-20. Hardness measurements were performed at a range of 500 μm on transversally cut samples. Tensile samples were prepared on wire erosion machine without harming the material structure in accordance with ASTM E8/E8M–11 standards. 3 pieces of tensile samples were prepared from each welded plates. Tensile tests were performed on Zwick100 tensile testing machine with a capacity of 10 tons.

3. Results and Discussion

3.1. Heat Distribution

Temperature values obtained from the thermocouple tips on the plates which were joined via FSW method at room temperature are graphically shown in Fig. 4. T2 and T4 values started to rapidly increase when the stir pin touched the material, and it reached a maximum value as soon as the shoulder touched the material. T2 and T1 positioned on the retreating side calculated temperature values as 162°C and 66°C, respectively. On the other hand, T4 and T3 on the advancing side measured temperature as 135°C and 51°C, respectively. The welding set continued to rotate in order to determine the necessary pre-heating temperature for FSW; however, it did not advance in order to cool the material. When all temperature values of thermocouple tips decreased to nearly 40°C, the welding set started to advance. While a sudden temperature rise was observed on T2 and T4, the temperature rise on T1 and T3 was relatively slow. Because the temperatures of welding set and material were low, no observable joint was apparent between the materials until T2 and T4 temperature values were nearly 183°C. No defects were seen on the seam surface, and a flawless joint was observed on the weld seam where T1, T2, T3 and T4 temperature values were nearly equal to 180°C. At the end of welding process, T1 and T3 temperature values were calculated as 300°C and 330°C, respectively. The temperature difference on the advancing and retreating sides on the start and end of weld was measured as 30°C. As can be seen on the graph, if the welding process had not been ended, average temperature value of the plates on the start and end of weld would have been 150°C and 310°C, respectively.

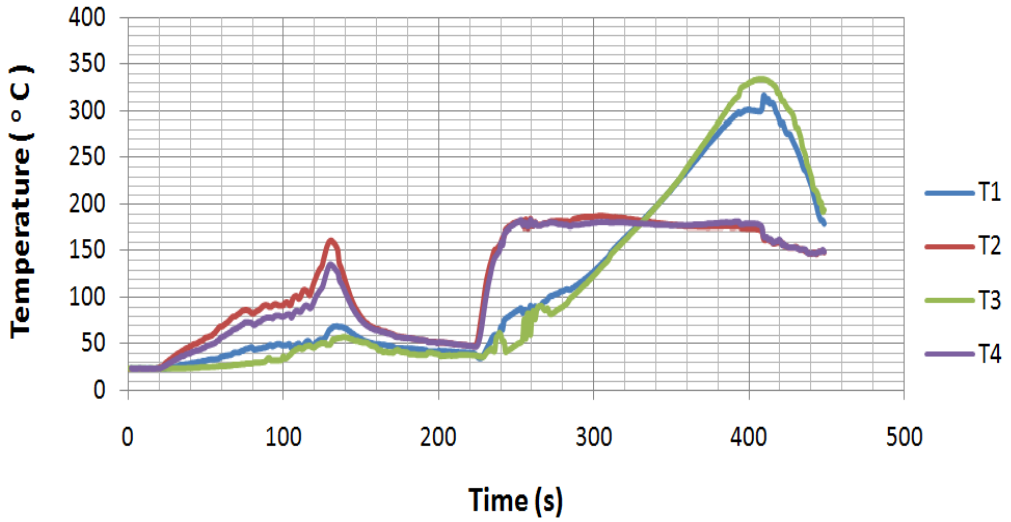

Figure 4. The heat distribution of Al7039 alloy joined via FSW

As the heat distribution graph of FSW at room temperature demonstrates, the heat distribution caused by the welding set over the base material around the weld zone causes a heat loss, which varies depending on the thermal conductivity of the materials joined via FSW. Since this heat loss influences welding process negatively and the joint was observable only at 183°C during FSW at room temperature, Al7039 material was annealed in the oven at 200°C for 30 minutes and tied to the bench for welding process. The heat distribution graph of welding process with the same welding parameters and thermocouple tips is shown in Fig. 5.

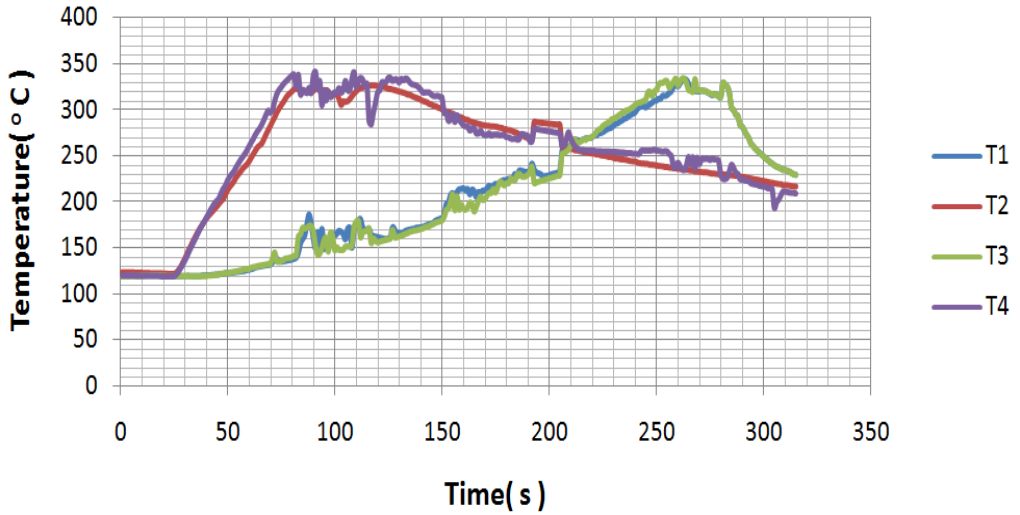

Figure 5. The heat distribution graph of Al7039 alloy joined via FSW following pre-heating

During the time that elapsed until the materials were tied to the bench, their temperatures on each zone prior to the welding process were calculated as nearly 120°C. While T2 and T4 temperature values displayed a sudden temperature rise up to 325°C after the shoulder touched the material, T1 and T3 temperature values increased to 167°C and 143°C, respectively. T2 and T4 temperature values were measured as 232°C and 246°C at the end of weld, respectively, while T1 and T3 temperature values were measured as nearly 321°C. As the graph also demonstrates, the temperature value remains the same at the beginning and end of welding process, which justifies the determined pre-heating temperature. During the welding process, another thermocouple measured the maximum temperature values on the weld zone and welding set as nearly 360°C and 420°C, respectively.

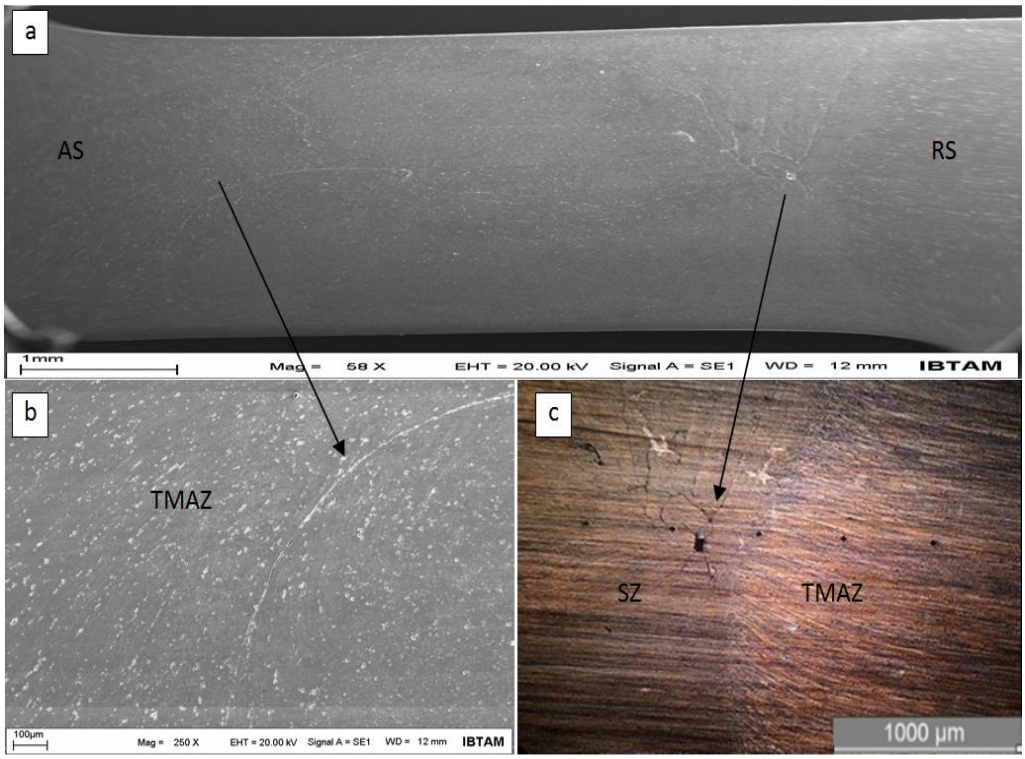

Figure 6. SEM and optical microscope images of the sample taken from start of seam between the plates joined via FSW at room temperature

3.2. Micro structure analysis

After observable joints were apparent on plates which were subjected to pre-heating and joined at room temperature, the samples taken from start, end and center of weld seam were prepared for micro structure analysis.

SEM and optical microscope images of the sample taken from the start of weld seam and overall view of the sample are shown in Fig. 6 and 6a, respectively. The joint defect observed on the line between thermo-mechanically affected zone (TMAZ) and stirring zone (SZ) on the advancing side is clearly shown in Fig. 6b. Additionally, the microscopic images of gaps and cracks were observed on SZ close to the retreating side are shown in detail in Fig. 6c. These defects can be associated with the insufficiency of the temperature for the materials. The incompatibility of the structure which reached a high temperature on SZ with that of Al7039 material which lost its heat due to its high thermal conductivity results from insufficient temperature. It must be noted that any insufficient heat input causes the welding process to encounter such defects.

The overall view of the samples taken from center and end of weld seams between the plates is given in Fig. 7, respectively. As shown in Fig. 7a, no joint defects are observed on the center of weld seam, resulting from the equal temperature (185^{o}C) at the start and end of the joint between the plates joined by the stirring pin which advanced to this zone during FSW. Although no important defects are observed on the overall view of the sample taken from the end of weld seam in Fig. 7, a further detailed analysis demonstrated that some slight joint defects called kissing bond could be found on the stirring zone of retreating side due to a lack of oxide layer cleaning on the material surface [18].

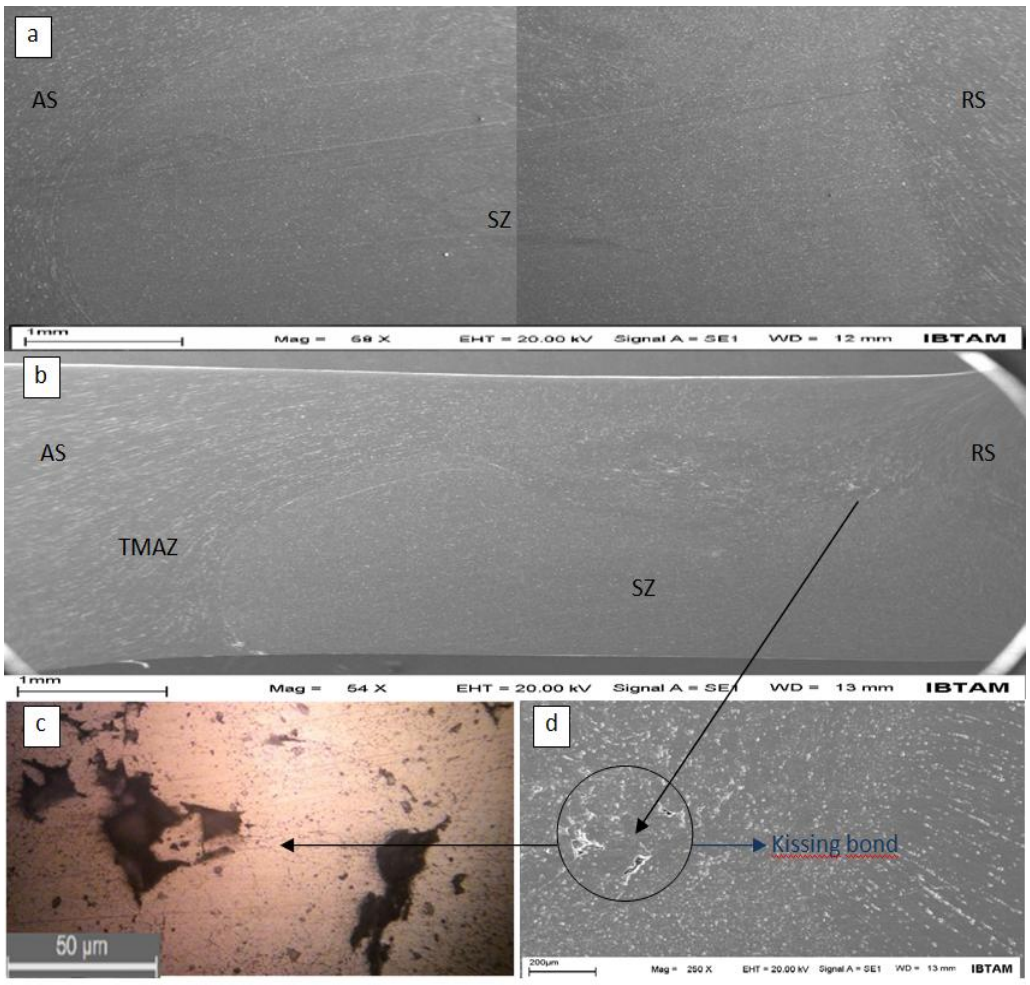

Figure 7. The plates joined via FSW at room temperature **a)** General SEM image of the center of seam **b)** General SEM image of the end of seam **c)** SEM image of kissing bond **d)** Microscope image of kissing bond

No defects were observed on the start and center of welds seams on the samples taken from the plates joined by applying pre-heating, thus displaying an excellent zonal formation. The micro structure images of SZ and TMAZ joint lines on advancing and retreating sides taken from these samples are given in Fig. 8a and 8b, respectively. It can be clearly observed that $MgZn_2$ precipitation in Al7039 material concentrated around SZ and joint lines due to pre-heating, particularly as homogenous and smaller quantities on SZ. In Fig. 8c, the micro structure image of the sample taken from the end of weld seam is shown to display SZ, TMAZ, heat-affected zone (HAZ) and base metal lines. Similar to FSW at room temperature, some slight kissing bonds are observed on the same zone due to FSW with pre-heating. It is possible to argue that the defect can be eliminated by removing oxide layer on the base metal thanks to pre-heating.

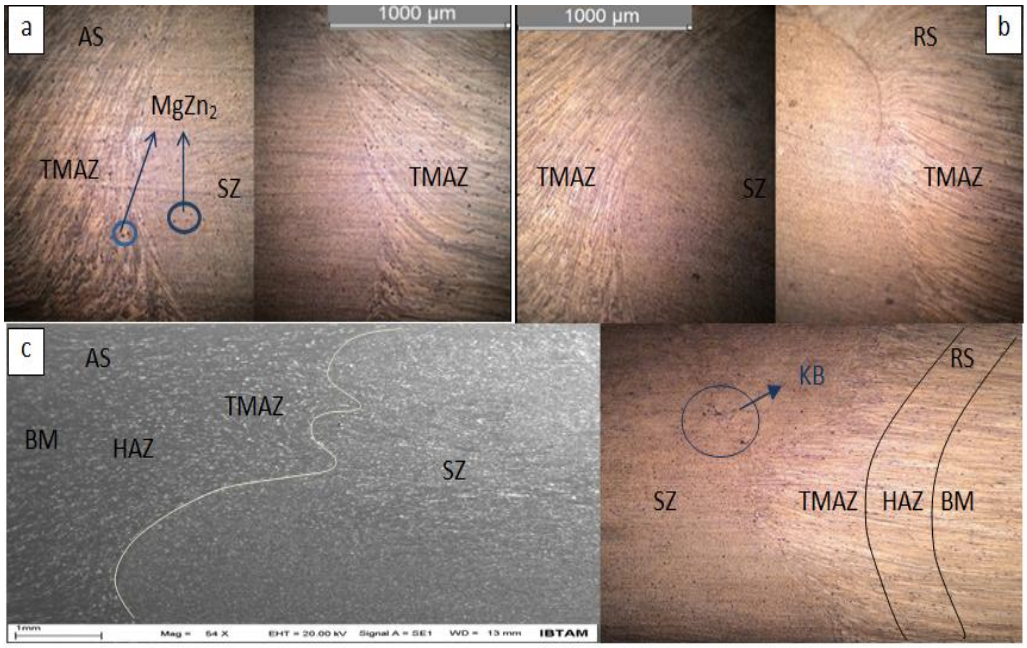

Figure 8. The plates joined via FSW following pre-heating **a)** The image of start of seam **b)** The image of center of seam **c)** The image of end of seam

According to EDX analysis on SZ, advancing and retreating sides and base metal, it was observed that Al_{13} Mg_{12} Zn_{30} preserved its integrity flawlessly, and that no intermetallic compound formed on any zone of the samples. EDX analysis results for SZ following FSW at room temperature are shown in Fig. 9.

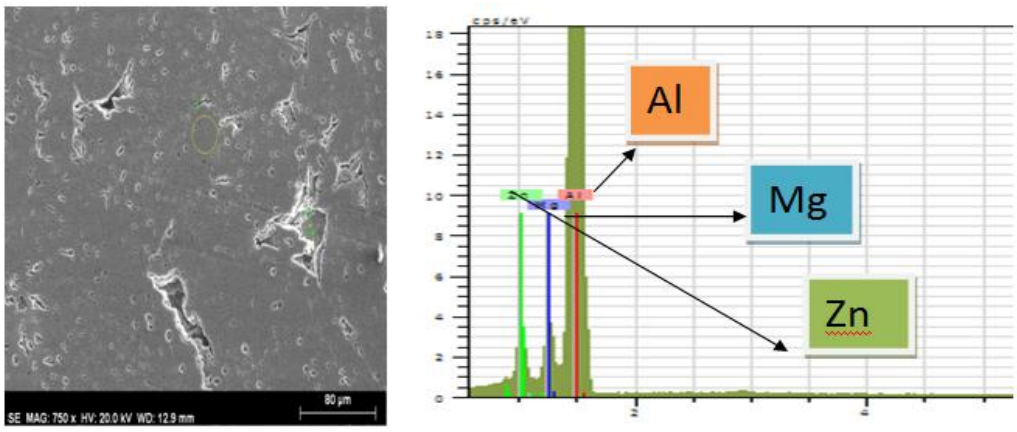

Fig.9. EDX analysis results of SZ

3.3. Micro Hardness Results

The results of the micro hardness test, which was conducted on start, end and center of weld seam for the samples joined via FSW at room temperature, are graphically shown in Fig. 10. For each seam zone, hardness samples were taken from reverse zones on the base metal, HAZ, TMAZ, SZ, and retreating and advancing sides. The black points, as shown in Fig. 6c, came into being following the hardness measurement.
The red line on the graph belongs to the sample taken from the center of weld seam where the temperature was equal at the start and end of the material. The hardness value, which was measured as 105 Hv on the center of SZ, increases as it advances towards TMAZ, and reaches 118 Hv for TMAZs on both advancing and retreating sides. On the other hand, the hardness of HAZs on both sides displayed an equally slight decline, which was measured nearly as 115 Hv. In general, the hardness values of this sample were evidently close for each zone.

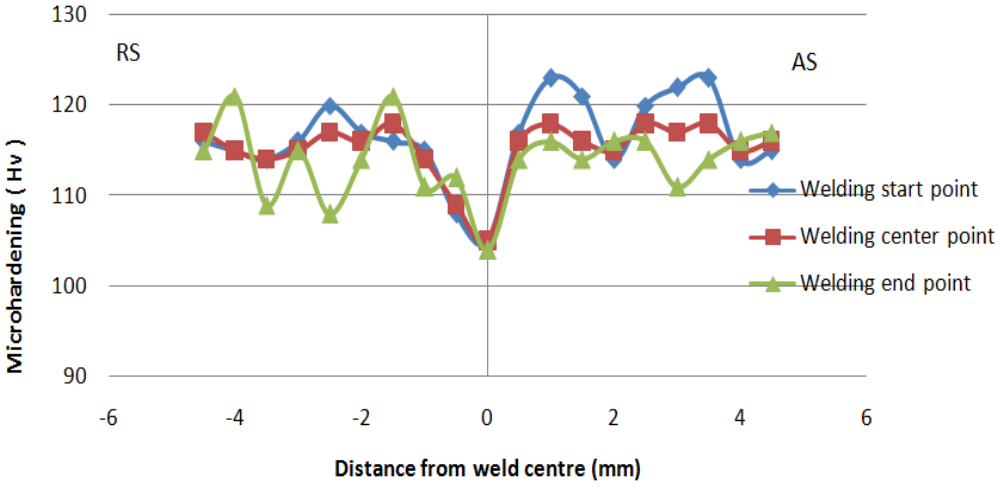

Figure 10. Micro hardness results of the plates joined via FSW at room temperature

When the blue line representing the sample taken from the start of weld seam is analyzed, the average hardness values of TMAZ on retreating and advancing sides were nearly 118 Hv and 124 Hv, respectively. On the other hand, the hardness value of HAZ was measured as 114 Hv. While the average hardness values of TMAZs on both retreating and advancing sides on the end of weld seam were calculated as 121 Hv and 116 Hv, respectively, it was calculated as 110 Hv for HAZs. It can be safely argued that the low temperature on the advancing side compared to the retreating side for the start of the weld seam increased the hardness value of TMAZ, while a contrary situation was valid for the end of weld seam, which resulted in a higher TMAZ hardness.

The results of the micro hardness test, which was conducted on the start, end and center of seam for the samples joined via FSW with pre-heating, are graphically shown in Fig. 11. The average hardness values of TMAZ on both retreating and advancing sides of the sample taken from the center of weld seam were calculated as 116 Hv and 118 Hv, respectively, while the same values were calculated as 115 Hv on HAZ and 105 Hv on SZ. The average hardness value on SZ are nearly the same for each sample. The average hardness values of TMAZs on both retreating and advancing sides of the sample taken from the start of weld seam were calculated as 113 Hv and 115 Hv, respectively. On the other hand, the same values were calculated as 117 Hv and 111 Hv for HAZ on both retreating and advancing sides, respectively. Finally, the average hardness values of TMAZs on both retreating and advancing sides of the sample taken from the end of weld seam were calculated as 116 Hv and 113 Hv, respectively, while it was calculated as 112 Hv for HAZs on both sides.

Given that the average hardness value of the main sample after the applied processes was 115 Hv, it can be concluded that the hardness value of all samples did not change considerably following FSW with pre-heating.

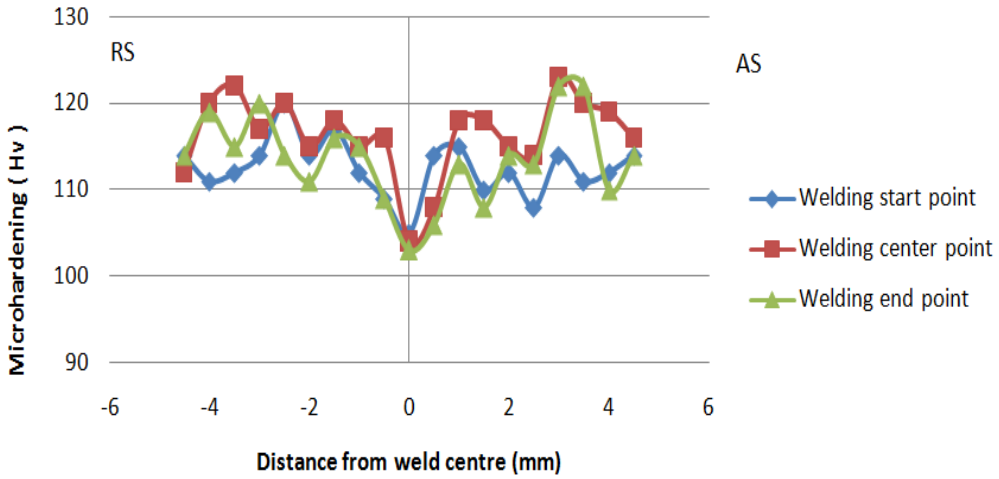

Fig.11. Micro hardness results of the plates joined via FSW following pre-heating

3.4. Tensile Test Results

As shown in Figure 12a, a flawless rear joint was observed on the back surfaces of both samples following FSW. However, chip samples were taken from both surfaces of the sample in order to remove burrs on the weld surface in order to eliminate any misleading results related to the tensile test, and, as shown in Fig. 12b, the thickness of the samples were reduced to 4 mm. The sample joined at room temperature, the sample joined using pre-heating and the sample Al7039 which was not welded were cut on the wire erosion machine at the dimensions given in Fig. 13. Three tensile samples were taken from the start, center and end of weld seams on both welded samples. On the other hand, three samples taken from the base sample which was not welded were compared to the welded samples. The results of the tensile test are graphically in Fig. 14.

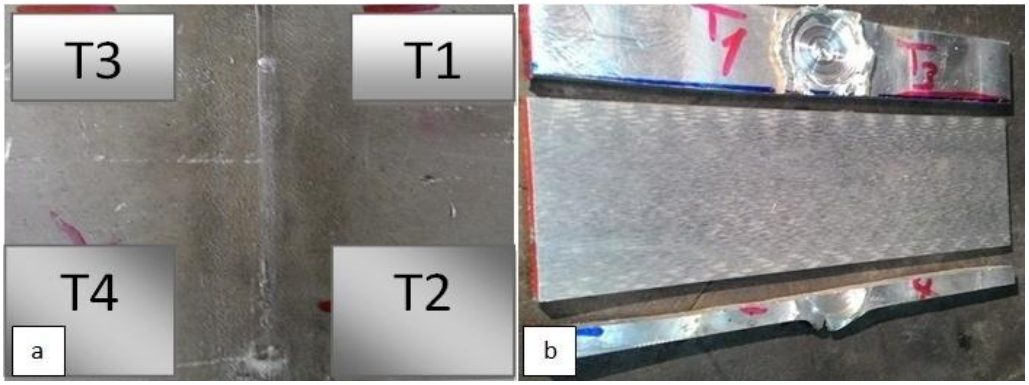

Fig.12. a) Rear joint following the welding process **b)** Cleaning of samples prior to tensile test

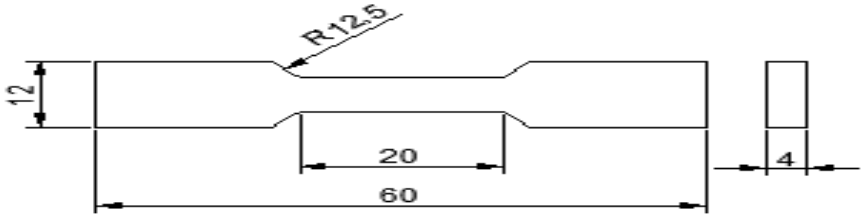

Fig.13. Tension sample size (mm)

When it comes to the samples taken following FSW at room temperature, the highest tensile strength was observed on the center and end of weld seam as 267 MPa, while the same value was calculated as 231 MPa on the start of weld seam. As for the samples taken following FSW with pre-heating, on the other hand, the highest tensile strength belonged to the start of weld seam as 381 MPa, while it was 358 MPa and 340 MPa on the end and center of weld seam, respectively.

The average tensile strength of the samples taken from the base metal was 429 MPa, demonstrating that the tensile strength and toughness of the base metal converge to the base metal thanks to the pre-heating when the joining methods are compared.

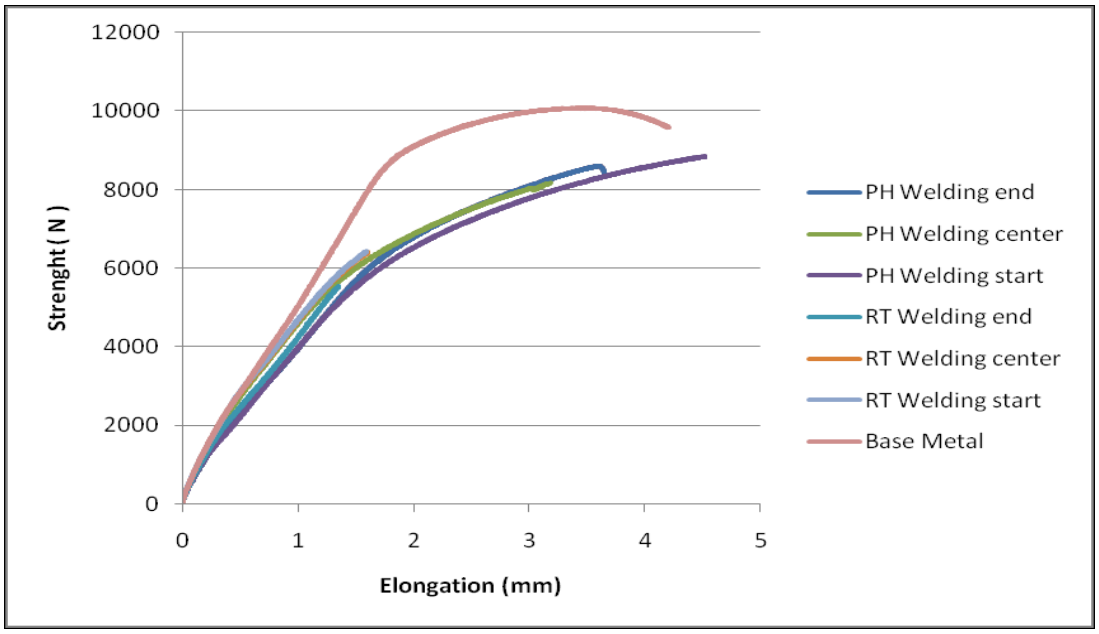

Figure 14. The tensile test of the samples taken following FSW with pre-heating and FSW at room temperature

4. Conclusion

Various problems are encountered during a welding process due to the heat distribution, particularly when the materials with high thermal conductivity are joined. Since FSW, too, poses such problems, this study aimed to join Al7039 alloy plates via FSW method at room temperature and with pre-heating and determine the necessary temperature during these processes thanks to the thermocouples positioned at start and end of weld. Thus, the impact of the values on the materials joined via FSW was analyzed.

1. The welding set used to determine the pre-heating temperature during FSW at room temperature continued to rotate after it penetrated the material; however, it did not advance. When the temperature was 40^{o}C at all zones of the material, the welding set advanced to observe the impact of heat distribution on the apparent joint. Although no joint was observed until the temperature was 183^{o}C at the start of the plate, it was later found out that the most effective joint was apparent on the start and end of the plate where the temperature was equal to 180^{o}C. Then, the plates were tied to the joining apparatus and annealed in the oven for pre-heating at 200^{o}C for 30 minutes. However, during the time that elapsed until the materials were tied to the bench, the temperature on the start and end of the plates were 120 ^{o}C.
2. The micro structures of the samples taken from the start, center and end of weld seam were analyzed after an apparent joint was observed for both FSW at room temperature and with

pre-heating. During FSW at room temperature, a welding defect occurred on the line between TMAZ and SZ on the advancing side as well as some cracks and gaps on the retreating side due to the insufficiency of the heat distribution on the start of weld. Although no defects were observed on the center of weld seam, kissing bonds were apparent on SZ which is close to TMAZ on the end of weld seam of advancing side due to a lack of oxide layer cleaning on the material surface. On the other hand, during FSW with pre-heating, no defects were observed on the start and center of weld seam. However, kissing bonds could be seen on the end of weld seam on the same zone. EDX analysis indicated that no intermetallic compounds occurred and that $MgZn_2$ distribution on weld zones were more homogenous following pre-heating.

3. It was found out in the tensile test that the samples on the zones where $MgZn_2$ distribution was homogenous displayed remarkably close tensile strengths following pre-heating. On the other hand, FSW at room temperature led to more varying tensile strengths.
4. When the tensile test results were analyzed following FSW, it was demonstrated that pre-heating increased the toughness of the material and improved tensile strength by 40%, which may result from the suitability of the heat distribution over the plates.

References

[1] Rometsch P. A., Zhang Y., Knight S. “Heat treatment of 7xxx series aluminium alloys - Some recent developments,” *Transactions of Nonferrous Metals Society of China (English Edition)*, 2014, vol. 24, no. 7: pp. 2003–2017.

[2] Ludtka G. M., Laughlin D. E. “The Influence of Microstructure and Strength on the Fracture Mode and Toughness of 7XXX Series Aluminum Alloys” *Metallurgical Transactions A, 1982* vol. 13A : pp. 411-425.

[3] Avci U., Temiz Ş. “A new approach to the production of partially graded and laminated composite material composed of SiC-reinforced 7039 Al alloy plates at different rates,” *Composites Part B: Engineering*, 2017, vol. 131: pp. 76–81.

[4] Pérez-Bergquist S. J., Gray G. T. R., Cerreta E. K., Trujillo C. P., Pérez-Bergquist A. “The dynamic and quasi-static mechanical response of three aluminum armor alloys: 5059, 5083 and 7039,” *Materials Science and Engineering A*, 2011, vol. 528, no. 29–30 :pp. 8733–8741.

[5] Maleki E. “Artificial neural networks application for modeling of friction stir welding effects on mechanical properties of 7075-T6 aluminum alloy,” *IOP Conference Series: Materials Science and Engineering, 4th Global Conference on Materials Science and Engineering (CMSE 2015)*, vol. 103: pp. 1-15, (2015).

[6] Kurt H. I. “Influence of hybrid ratio and friction stir processing parameters on ultimate tensile strength of 5083 aluminum matrix hybrid composites,” *Composites Part B: Engineering*, 2016, vol. 93 : pp. 26–34.

[7] Seidel T. U., Reynolds A. P. “Visualization of the material flow in AA2195 friction-stir welds using a marker insert technique,” *Metallurgical and Materials Transactions A*, 2001, vol. 32, no. 11: pp. 2879–2884.

[8] Reynolds A. P. “Visualisation of material flow in autogenous friction stir welds,” *Science and Technology of Welding and Joining*, 2000, vol. 5, no. 2 : pp. 120–124.

[9] Peel M., Steuwer A., Preuss M., Withers P. J. “Microstructure, mechanical properties and residual stresses as a function of welding speed in aluminium AA5083 friction stir welds,” *Acta Materialia*, 2003, vol. 51, no. 16 : pp. 4791–4801.

[10] Singh R. K. R., Sharma C., Dwivedi D. K., Mehta N. K., Kumar P. “The microstructure and mechanical properties of friction stir welded Al-Zn-Mg alloy in as welded and heat treated conditions,” *Materials and Design*, 2011, vol. 32, no. 2 : pp. 682–687.

[11] K. Kumar and S. V. Kailas, “On the role of axial load and the effect of interface position on

the tensile strength of a friction stir welded aluminium alloy," *Materials and Design*, 2008, vol. 29, no. 4, pp. 791–797.

[12] Cavaliere P., Campanile G., Panella F., Squillace A. "Effect of welding parameters on mechanical and microstructural properties of AA6056 joints produced by Friction Stir Welding," *Journal of Materials Processing Technology*, 2006, vol. 180, no. 1–3 : pp. 263–270.

[13] Sharma C., Dwivedi D. K., Kumar P. "Influence of pre-weld temper conditions of base metal on microstructure and mechanical properties of friction stir weld joints of Al-Zn-Mg alloy AA7039," *Materials Science and Engineering A*, 2014, vol. 620 : pp. 107–119.

[14] Aydın H., Bayram A., Uğuz A., Akay K. S. "Tensile properties of friction stir welded joints of 2024 aluminum alloys in different heat-treated-state," *Materials & Design*, 2009, vol. 30, no. 6 : pp. 2211–2221.

[15] Chen Y., Liu H., Feng J. "Friction stir welding characteristics of different heat-treated-state 2219 aluminum alloy plates," *Materials Science and Engineering A*, 2006, vol. 420, no. 1–2 : pp. 21–25.

[16] Yan J., Reynolds A. P. "Effect of initial base metal temper on mechanical properties in AA7050 friction stir welds," *Science and Technology of Welding and Joining*, 2009, vol. 14, no. 4 : pp. 282–287.

[17] Poongkundran R., Senthilkumar K. "Effect of preheating on microstructure and tensile properties of friction stir welded AA7075 aluminium alloy joints," *Brazilian Archives of Biology and Technology*, 2016, vol. 59 : pp. 1–15.

[18] Khan N. Z., Siddiquee A. N., Khan Z. A., Shihab S. K. "Investigations on tunneling and kissing bond defects in FSW joints for dissimilar aluminum alloys," *Journal of Alloys and Compounds*, 2015, vol. 648: pp. 360–367.